Interactions between surfaces in the presence of nonadsorbing equilibrium polymers

2003 J. Phys.: Condens. Matter 15 6627

(http://iopscience.iop.org/0953-8984/15/40/002)

INSTITUTE OF PHYSICS PUBLISHING JOURNAL OF PHYSICS: CONDENSED MATTER

J. Phys.: Condens. Matter **15** (2003) 6627–6645 PII: S0953-8984(03)66380-0

Interactions between surfaces in the presence of nonadsorbing equilibrium polymers

J van der Gucht and N A M Besseling

Dutch Polymer Institute/Wageningen University, Laboratory of Physical Chemistry and Colloid Science, Dreijenplein 6, 6703 HB Wageningen, The Netherlands

E-mail: jasper.vandergucht@wur.nl

Received 17 July 2003
Published 26 September 2003
Online at stacks.iop.org/JPhysCM/15/6627

Abstract

The behaviour of a solution of equilibrium polymers (or living polymers) between two surfaces is studied using a Bethe–Guggenheim lattice model for molecules with orientation-dependent interactions. The average monomer concentration, the average length of the chains and the interaction between the surfaces are calculated as a function of the separation distance between the surfaces. When the gap is in full equilibrium with a homogeneous bulk solution, the equilibrium polymers cause a depletion attraction, which becomes stronger with increasing bulk monomer concentration. The range of the interaction passes through a maximum as a function of the concentration. In dilute solutions the range of the interaction increases and the strength decreases with increasing bonding energy, while above the overlap concentration the bonding energy is irrelevant. For restricted equilibrium between the gap and the bulk, when the amount of polymer in the gap is determined by the flow of fluid out of the gap upon compression, the interaction becomes repulsive. This repulsion becomes stronger with increasing concentration and depends only very weakly on the bonding energy. Two limiting cases for the fluid flow were considered: (i) perfect-slip conditions at the surfaces, resulting in a constant monomer concentration in the gap and (ii) no-slip conditions at the surfaces, resulting in a parabolic flow profile of solution out of the gap.

1. Introduction

It is well known that nonadsorbing polymers can cause phase separation in colloidal suspensions [1–11]. The origin of this effect, termed depletion flocculation, is the decrease in conformational entropy that a chain suffers when it is confined between two particles that are not too far apart. For nonadsorbing polymers this entropy loss is not compensated by an adsorption energy, so that polymers tend to avoid the region between the two particles. As a

result, the osmotic pressure between the particles is lower than in the bulk and the particles are pushed together. If this effect is strong enough, flocculation or phase separation is observed.

Several theoretical models have been proposed to describe the effect of nonadsorbing polymers on colloidal interactions. The first theoretical treatment was given by Asakura and Oosawa [1, 2]. These authors treated the polymer coils as hard spheres for the colloidal particles, and as penetrable spheres for other polymer coils. Each particle is then surrounded by a depletion zone with a thickness equal to the radius of gyration of the polymers. Overlap of the depletion zones is favourable, because this results in an increase of the total volume available for the polymers. This is the driving force for depletion phase separation. Joanny *et al* [4] used scaling arguments and mean-field calculations to extend the theory of polymer depletion to semi-dilute polymer solutions. In this case the thickness of the depletion layer corresponds to the correlation length ξ of the polymer solution, which is a decreasing function of the polymer concentration [3, 6, 12]. Scheutjens and Fleer [6–8] developed a self-consistent-field lattice theory, which proved to be successful in describing polymer adsorption and depletion. The density profile of polymers between two solid surfaces is evaluated and the interaction free energy between the surfaces is calculated as a function of the separation distance. Both for adsorbing and nonadsorbing polymers this interaction is attractive as long as the solution between the surfaces is in full equilibrium with an external reservoir with constant composition. The strength and range of the attraction depend on the chain length and polymer concentration.

The theoretical description of polymers at surfaces has focused mainly on monodisperse polymers. Polydisperse chains have received only very little attention [13–15]. In this paper we consider a special class of polymers, in which the bonds between monomers are not covalent, but are based on reversible interactions. Such chains are called equilibrium polymers (or 'living polymers' or 'supramolecular polymers'). Examples of equilibrium polymers are wormlike micelles [16] and supramolecular polymers based on hydrogen bonding [17–19]. The difference with classical polymers is that the bonds between the segments can break and recombine on experimental timescales. As a result, the chain length distribution in such systems is not fixed but is determined by thermodynamic equilibrium and responds to variable conditions. The equilibrium distribution can be calculated using statistical mechanics. Within a mean-field approximation, an exponential chain length distribution is predicted [16, 20, 21]:

$$\phi(N) = N\frac{\phi_{\mathrm{M}}}{\langle N_0\rangle^2}\exp\left(-\frac{N}{\langle N_0\rangle}\right) \tag{1}$$

where $\phi(N)$ is the volume fraction of chains of N segments, ϕ_{M} is the total volume fraction of monomers and $\langle N_0\rangle$ is the number averaged chain length. The factor $\phi_{\mathrm{M}}/\langle N_0\rangle^2$ normalizes the distribution, ensuring $\sum_N \phi(N) = \phi_{\mathrm{M}}$. The average chain length is a function of the monomer concentration ϕ_{M}, the scission energy E that is needed to break a bond between two monomers and the temperature T:

$$\langle N_0\rangle \simeq \phi_{\mathrm{M}}^{1/2}\exp\left(\frac{E}{2kT}\right) \tag{2}$$

where k is Boltzmann's constant. This equation is valid for $\langle N_0\rangle \gg 1$. The properties of a solution of equilibrium polymers can be 'tuned' by changing the monomer concentration or the temperature, by influencing the scission energy E (for example, by changing the solvent conditions) or by applying an external field such as a shear field.

Relatively little is known about the effect of equilibrium polymers on the interactions between colloidal particles. Schmitt *et al* [22] presented an analytical model for a dilute solution of ideal equilibrium polymer chains confined between two repulsive walls. Excluded volume interactions were not accounted for in this approach. These authors considered both the case where the solution in the gap is in full equilibrium with a reservoir, and a case

of restricted equilibrium where the volume fraction of polymers in the gap and the volume of the gap remain constant. In the former case, the interactions are attractive, while in the latter case a repulsion was predicted. Milchev and Landau [23] did lattice Monte Carlo simulations on concentrated solutions of equilibrium polymers confined between two surfaces. Their results show that the surface region is preferentially occupied by short chains, which is in agreement with the results for polydisperse systems of unbreakable polymers [14, 15]. Rouault and Milchev [24] used the same Monte Carlo algorithm to calculate the average chain length in a concentrated equilibrium polymer solution in a gap between two surfaces as a function of the gap size. In a recent paper [25] we applied a lattice theory for molecules with orientation-dependent interactions, originally developed to describe the structure of water [26], to a solution of equilibrium polymers at a single surface. In this model, correlations due to interactions between monomers are accounted for in a Bethe–Guggenheim (or quasi-chemical) approximation. Excluded volume interactions are accounted for by allowing only one molecule on each lattice site. We calculated the thickness of the depletion layer as a function of the polymer concentration and the scission energy. The depletion layer thickness passes through a maximum as a function of the monomer concentration. In dilute solutions the depletion layer thickness is proportional to the average radius of gyration of the chains, which increases with concentration as $\langle R_g \rangle \sim \langle N_0 \rangle^{1/2} \sim \phi_M^{1/4}$ within a mean-field approximation (see equation (2)). Above the overlap concentration, the depletion layer thickness is proportional to the correlation length ξ, which decreases with increasing concentration as $\xi \sim \phi_M^{-1/2}$ within the mean-field approximation (the so-called marginal regime). We also calculated the distribution of chain lengths near the surface and found that the surface region is predominantly occupied by the shorter chains.

In this paper, we extend these results to a solution of equilibrium polymers confined between two flat surfaces. We calculate the average concentration in the gap and the average length of the chains as a function of the separation distance between the surfaces. Furthermore we calculate the interaction free energy between the surfaces. For describing the interactions between two surfaces, the thermodynamic conditions under which the surfaces approach is crucial. Clearly, this depends on the ratio of the timescale of the approach of the surfaces and the timescale of the diffusion of polymers. Here, we consider both the case of *full equilibrium* and that of *restricted equilibrium*. In the first case the solution in the gap is always in equilibrium with a bulk solution, implying a constant chemical potential. This situation applies when the approach between the two surfaces is sufficiently slow for equilibrium between the bulk and the gap to be maintained. This is generally assumed to be relevant for describing depletion interactions in colloidal dispersions where the collision time of particles due to Brownian encounters is usually relatively large compared to the diffusion time of the polymers.

On the other hand, if the time needed for polymers to diffuse out of the gap is large compared to the timescale of approach between the surfaces, then full equilibrium with the bulk will not be maintained. This will be the case for a relatively fast compression of a narrow gap between two plates of large surface area. In this case, the chemical potentials inside the gap and in the bulk are no longer equal. A statistical thermodynamic treatment is still possible if some additional assumptions are made about the polymer concentration in the gap and about the redistribution of monomers in the overlap region of the two depletion layers. Here, we will assume that diffusion of polymers from the gap to the bulk and vice versa is negligible. Variations of the amount of polymer in the gap are determined only by the fluid flow out of the gap when the surfaces are moved closer together and thus depend on the velocity profile of the fluid flow. We furthermore assume that, for the given amount of polymer in the gap, local equilibrium is maintained in the direction normal to the surfaces (i.e. the redistribution of monomers in the normal direction is assumed to be very rapid). The concentration in

the lateral direction remains homogeneous for this case. This situation applies when the timescale on which the surface separation is varied is much larger than the time needed for the polymers to diffuse over a distance comparable to the gap width, but much smaller than the time needed for diffusion out of the gap. This is the case for narrow gaps between large surfaces. Furthermore the variation of the surfaces should be slow compared to the kinetics of breaking and recombination of bonds between monomers.

We note that diffusion may be faster for equilibrium polymers than for covalent polymers of the same length, because the chains can break and recombine. Hence, full equilibrium may be more easily obtained for equilibrium polymers than for ordinary polymers, which may be advantageous in experiments [27].

The thermodynamics of interactions between two surfaces are described in section 2.1, and in section 2.2 we describe the lattice model for calculating the concentration profile of monomers in the gap and the interactions between the surfaces. The case of full equilibrium between the gap and the bulk is considered in section 3. In section 4 we consider restricted equilibrium. Two different approaches, based on two limiting cases for the fluid flow profile, are described to calculate variations in the amount of polymer in the gap.

2. Theory

2.1. Interactions between two surfaces

We consider two solid plates of area A immersed in a solution of equilibrium polymers at constant pressure p and temperature T. The total amount of molecules n_A (where the subscript A denotes either a monomer or a solvent molecule) is fixed for all components A. The Gibbs free energy G of this system is given by

$$G(\{n_A\}p, T) = \sum_A n_A^g \mu_A^g + \sum_A n_A^b \mu_A^b + 2\gamma A \tag{3}$$

where μ_A is the chemical potential of component A, and γ is the surface tension at the inside of the gap (which depends on the surface separation h). The superscript g denotes molecules in the gap and the superscript b molecules in the bulk. Obviously, because the total amount of monomers and solvent molecules in the system is fixed, we have $n_A^b + n_A^g = n_A$. We assume furthermore that the bulk is infinitely large so that transport of molecules from the gap to the bulk or vice versa does not change the composition of the bulk. Hence, the chemical potentials in the bulk and the concentration profiles at the outside of the gap are constant. Therefore also the interfacial tension at the outer surfaces of the plates is constant and can be disregarded.

The quantity of interest is the free energy change per unit area when the plates are brought from infinite separation towards a separation h:

$$\Delta G(h) = G(h) - G(\infty). \tag{4}$$

If the system is in full thermodynamic equilibrium, the chemical potentials in the bulk and in the gap are equal. In this case the sum of the first two terms in equation (3) is constant at all separations h, so that the free energy of interaction is simply given by the change in the interfacial free energy:

$$\Delta G^{fe}(h) = 2A[\gamma(h) - \gamma(\infty)] \tag{5}$$

where the superscript fe stands for full equilibrium. As explained in the introduction, for this situation to occur, the molecules in the gap should be able to diffuse out of the gap on the timescale of variation of the distance between the two surfaces. If this is not the case, full equilibrium between the gap and the bulk cannot be maintained and the chemical potential in

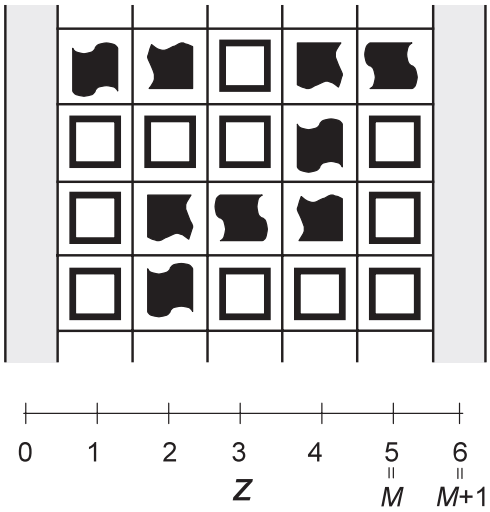

Figure 1. A two-dimensional representation of a three-dimensional cubic lattice. At layers $z = 0$ and $M + 1$ there are solid surfaces. Layers 1 to M contain solvent molecules (open squares) or bifunctional monomers (filled figures). The bonding groups of the monomers are represented as curved edges.

the gap differs from that in the bulk. For that case also the first two terms in equation (3) must be taken into account. The variation of the amount of molecules in the gap is now not (only) determined by thermodynamics, but also by the flow of fluid out of the gap as the surfaces are brought together (see section 4).

2.2. Bethe–Guggenheim lattice theory

In order to calculate the density profiles of monomers in the gap, we use a self-consistent-field lattice theory for molecules with interactions that depend on their relative orientations. The theory was developed by Besseling and Scheutjens to describe the structure of water and hydration forces [26, 28, 29]. Recently, we applied it to a system of equilibrium polymers [25]. In this section we describe the general features of the model. A more detailed description can be found in [26] and [25].

A schematic representation of the model is depicted in figure 1. The volume between the two surfaces is divided into a number of identical lattice sites. Each site contains either a solvent molecule or a bifunctional monomer. The lattice is divided into M parallel lattice layers, numbered $z = 1, 2, \ldots, M$. At layers $z = 0$ and $M + 1$ there is a solid surface. The distance between the surfaces is $h = Ml$, where l is the lattice spacing. The number of sites in each layer is denoted L and the area of the surfaces is $A = aL$ with a the cross-sectional area of a lattice site. The surface area, and hence L, are taken to be infinitely large, so that edge effects can be ignored. The lattice coordination number q gives the number of neighbouring sites that each lattice site has. As in [25], in this paper we use a cubic lattice, in which $q = 6$. Four of these neighbouring sites are within the same lattice layer.

The surface of each molecule consists of q faces that are directed towards nearest-neighbour sites. A bifunctional monomer has two different types of faces. Two of its q faces are the bonding groups (in figure 1 represented as curved edges) and the remaining $q - 2$ faces are non-bonding faces. A monomer can have a number of different monomeric states.

The state of a monomer is specified by the direction in which the two bonding groups are pointing. In the present paper we consider only completely flexible chains. Hence, there is no energy difference between linear states in which the two bonding groups are on opposite sides of the monomer and bent states where the two bonding groups make a 90° angle. The solvent molecules are isotropic, because all q faces of a solvent molecule are identical. Solvent molecules therefore have no distinguishable states.

The number of molecules of type A having state σ that are located at layer z is denoted $n_{\mathrm{A}}^{\sigma}(z)$. Here the subscript A denotes either a monomer (M) or a solvent molecule (S). Every lattice site is occupied by either a monomer or a solvent molecule, so that the following constraint needs to be satisfied:

$$\sum_{\mathrm{A}} n_{\mathrm{A}} = n_{\mathrm{M}} + n_{\mathrm{S}} = ML \tag{6}$$

where $n_{\mathrm{A}} = \sum_{\sigma,z} n_{\mathrm{A}}^{\sigma}(z)$ is the total number of molecules of type A in the system. The number of faces of type α in layer z, pointing in direction d, is denoted $n_{\alpha}^{d}(z)$. Obviously, the distribution of faces is directly related to the distribution of molecule states. The number of contacts between faces of type α with direction d at sites in layer z and faces of type β is denoted $n_{\alpha\beta}^{d}(z)$. One of these contact types (between two bonding groups) denotes the formation of bonds between monomers. Obviously, the following relation should hold for the distribution of contacts:

$$\sum_{\beta} n_{\alpha\beta}^{d}(z) = n_{\alpha}^{d}(z) \tag{7}$$

for all α, z and d.

A Bethe–Guggenheim or quasi-chemical approximation is used to calculate the occupation of the lattice sites. Correlations between neighbouring sites are accounted for in this approach, but pairs of sites are occupied independently. Within this approximation, the distribution of contacts between faces of type α and faces of type β depends on the contact energy $u_{\alpha\beta}$ between these faces. The following equation has been derived for the contact distribution [26]:

$$\phi_{\alpha\beta}^{d}(z) = \frac{\phi_{\alpha}^{d}(z)\phi_{\beta}^{-d}(z+\underline{d})}{G_{\alpha}^{d}(z)G_{\beta}^{-d}(z+\underline{d})} \exp\left(-\frac{u_{\alpha\beta}}{kT}\right). \tag{8}$$

Here $\phi_{\alpha}^{d}(z) \equiv n_{\alpha}^{d}(z)/L$ and $\phi_{\alpha\beta}^{d}(z) \equiv n_{\alpha\beta}^{d}(z)/L$ are the site fractions of faces and contacts. The direction indicated $-d$ is the opposite of d, and $z+\underline{d}$ denotes the layer at which d is directing from layer z (here $\underline{d}$ can have the values -1, 0 or 1). The factors $G_{\alpha}^{d}(z)$ and $G_{\beta}^{-d}(z+\underline{d})$ are face weighting factors, accounting for the saturation of faces. They are determined by constraint (7). From equation (8) we see that low-energy contacts are favoured over high-energy ones. This is different from the Bragg–Williams or random-mixing approximation, for which the occupancy of nearest-neighbour sites is stochastically independent: $\phi_{\alpha\beta}^{d*}(z) = \phi_{\alpha}^{d}(z)\phi_{\beta}^{-d}(z+\underline{d})$ (here the asterisk denotes a random distribution of contacts).

A bond between two monomers is formed if two bonding groups point towards each other. The strength of such a bond is determined by the contact energy $-E$ between two bonding groups. If E is large, bonds are very favourable and long chains will be formed. Here, we take the contact energies between other combinations of faces (of monomers and solvent) equal to zero. Hence, $u_{\alpha\beta} = -E$ if α and β are both bonding groups and $u_{\alpha\beta} = 0$ otherwise. All interaction energies with the surface are set to zero as well, so there is no preferential interaction of either monomers or solvent with the surface.

For the distribution of molecules over the lattice layers the following equation has been derived [26]:

$$\phi_{\mathrm{A}}^{\sigma}(z) = \Lambda_{\mathrm{A}} G_{\mathrm{A}}^{\sigma}(z) \tag{9}$$

where $\phi_{\mathrm{A}}^{\sigma}(z) \equiv n_{\mathrm{A}}^{\sigma}(z)/L$ is the fraction of sites in layer z occupied by molecules of type A in state σ, and where $\Lambda_{\mathrm{A}} = \exp(\mu_{\mathrm{A}}/kT)$ is a normalization constant, with μ_{A} the chemical potential of component A. Summation over all states σ and layers z yields the following expression for Λ_{A}:

$$\Lambda_{\mathrm{A}} = \frac{\theta_{\mathrm{A}}}{\sum_{\sigma,z} G_{\mathrm{A}}^{\sigma}(z)} \tag{10}$$

where θ_{A} is the amount of molecules of type A expressed in equivalent lattice layers: $\theta_{\mathrm{A}} = \sum_z \phi_{\mathrm{A}}(z)$ with $\phi_{\mathrm{A}}(z) = \sum_{\sigma} \phi_{\mathrm{A}}^{\sigma}(z)$ the volume fraction of monomers in layer z. Equation (10) makes it possible to normalize any component A by either fixing the chemical potential μ_{A} (full equilibrium conditions) or by fixing θ_{A} (restricted equilibrium).

The weighting factor $G_{\mathrm{A}}^{\sigma}(z)$ in equation (9) measures the probability of finding a molecule of type A in state σ in layer z. It can be factorized as

$$G_{\mathrm{A}}^{\sigma}(z) = C \prod_{\alpha,d} G_{\alpha}^{d}(z)^{q_{\mathrm{A}\alpha}^{\sigma d}} \tag{11}$$

where $q_{\mathrm{A}\alpha}^{\sigma d}$ equals 1 if the face pointing in direction d of a molecule A having state σ is of type α and zero otherwise. Each face of molecule A contributes a factor $G_{\alpha}^{d}(z)$ to $G_{\mathrm{A}}^{\sigma}(z)$. The factor C is a consequence of constraint (6). It can be shown that $C = 1$ in homogeneous systems, while for heterogeneous systems C is related to the interfacial tension γ [26]:

$$\frac{2\gamma a}{kT} = M \ln C. \tag{12}$$

The distribution of contacts and monomer states is completely determined by the self-consistent equations (8), (9) and the constraints (6) and (7). These equations can be solved numerically, as described in [26]. The distribution of chain lengths can then be calculated using the method described in [25]. The number average chain length can be calculated directly as

$$\langle N \rangle = \frac{\theta_{\mathrm{M}}}{\frac{1}{2}\sum_z \phi^{\mathrm{e}}(z)} \tag{13}$$

where $\theta_{\mathrm{M}} = \sum_z \phi_{\mathrm{M}}(z)$ is the total number of monomers between the plates and where $\phi^{\mathrm{e}}(z)$ denotes the number of end segments in layer z, i.e. the number of bonding groups in layer z that are not linked to another bonding group. The excess amount of monomers in the gap as compared to the bulk solution, expressed in equivalent lattice layers, is defined as

$$\theta^{\mathrm{ex}} = \sum_{z=1}^{M} (\phi_{\mathrm{M}}(z) - \phi_{\mathrm{M}}^{\mathrm{b}}) \tag{14}$$

where $\phi_{\mathrm{M}}^{\mathrm{b}}$ is the bulk volume fraction of monomers. If depletion occurs, θ^{ex} is negative. At infinite separation between the surfaces we may use θ^{ex} to obtain a measure for the depletion layer thickness at a single surface:

$$\Delta_1 = \frac{\theta^{\mathrm{ex}}(\infty)}{2\phi_{\mathrm{M}}^{\mathrm{b}}} \tag{15}$$

where the factor 2 accounts for the two surfaces.

3. Full equilibrium

In this section we consider a film containing equilibrium polymers and solvent between two surfaces in full equilibrium with the bulk of the solution. The equilibrium polymers do not adsorb on the surface. Hence, depletion layers will be formed near the two surfaces. The

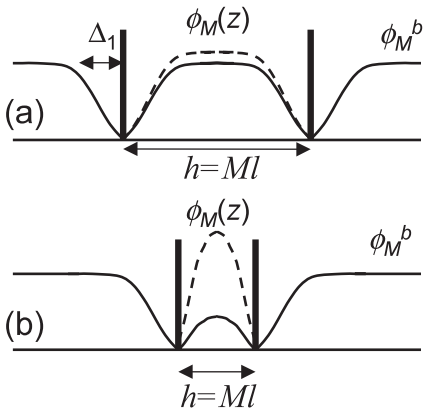

Figure 2. Depletion of equilibrium polymers between two plates. Schematic concentration profiles inside and outside the gap for large separations $h \gg \Delta_1$ (a) and for small separations $h < \Delta_1$ (b). The full curves refer to the case of full equilibrium with the bulk of the solution and the broken curves to restricted equilibrium with the bulk (see section 4).

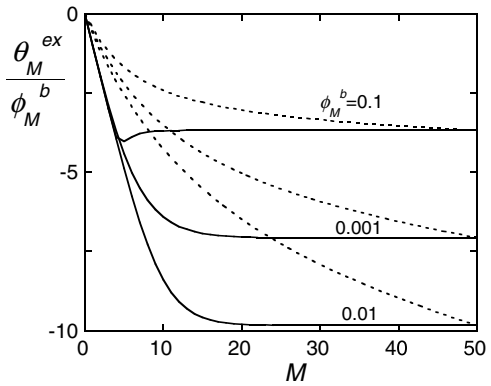

Figure 3. The excess amount of polymer between two plates immersed in a solution of flexible living polymers ($E = 15kT$) as a function of the separation distance for three different $\phi_{\mathrm{M}}^{\mathrm{b}}$. Full curves: full equilibrium, dotted curves: restricted equilibrium with no-slip conditions, $M' = 50$ (see section 4.2).

principle of depletion is illustrated in figure 2. Schematic concentration profiles of monomers at the inside and outside of the gap are shown for wide and narrow gaps (the full curves refer to full equilibrium). Near the two surfaces there are depletion zones (with a thickness Δ_1) where the segment concentration is lower than in the bulk of the solution. This is due to conformational restrictions that are, for nonadsorbing polymers, not compensated by an adsorption energy.

The excess amount of polymer θ^{ex} between the two surfaces is shown in figure 3 as a function of the separation distance M for monomers with a scission energy $E = 15kT$ for three different bulk concentrations. The full curves refer to the case of full equilibrium between the gap and the bulk. Figure 4 shows the average monomer concentration $\langle\phi_{\mathrm{M}}\rangle = \sum_z \phi_{\mathrm{M}}(z)/M$ in the gap for the same parameters. Obviously, the excess amount is negative for the present case of nonadsorbing polymers and $\langle\phi_{\mathrm{M}}\rangle/\phi_{\mathrm{M}}^{\mathrm{b}} < 1$. At large separations $M \gg \Delta_1$, when the depletion layers at the two surfaces do not overlap (figure 2(a)), θ^{ex} is constant and equal to

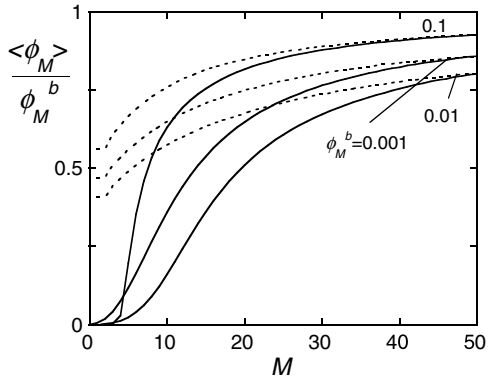

Figure 4. The average volume fraction of monomers in the gap as a function of the separation distance for $E = 15kT$ and three different $\phi_{\mathrm{M}}^{\mathrm{b}}$. Full curves: full equilibrium, dotted curves: restricted equilibrium with no-slip conditions, $M' = 50$ (see section 4.2).

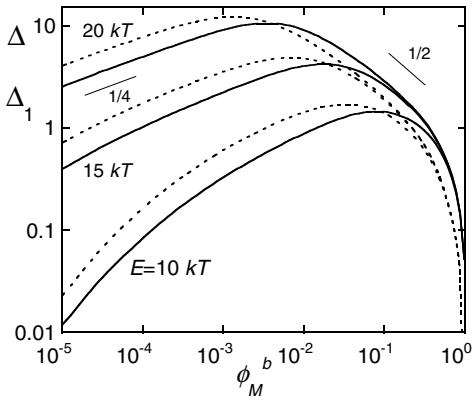

Figure 5. The depletion layer thickness at a single surface $\Delta_1 = \theta^{\mathrm{ex}}(\infty)/2\phi_{\mathrm{M}}^{\mathrm{b}}$ (dotted curves) and the range of the depletion interaction between two surfaces at full equilibrium Δ (full curves, see also figure 7) as a function of $\phi_{\mathrm{M}}^{\mathrm{b}}$ for several E.

twice the depleted amount at a single surface. The average volume fraction in this regime varies as $(\langle\phi_{\mathrm{M}}\rangle - \phi_{\mathrm{M}}^{\mathrm{b}}) \sim M^{-1}$. The depletion layer thickness Δ_1 (equation (15)) is shown in figure 5 as a function of the monomer concentration for three values of E (the broken curves). As discussed in detail in a previous paper [25], there are two regimes for Δ_1. At low concentrations it is proportional to the average radius of gyration $\langle R_{\mathrm{g}}\rangle$ of the chains, while above the overlap concentration it corresponds to the correlation length ξ of the solution (the mesh size of the network). Hence

$$\Delta_1 \sim \begin{cases} \langle R_{\mathrm{g}}\rangle \sim \langle N_0\rangle^{1/2} \sim (\phi_{\mathrm{M}}^{\mathrm{b}})^{1/4} \exp\left(\dfrac{E}{4kT}\right) & \text{for } \phi_{\mathrm{M}}^{\mathrm{b}} < \phi_{\mathrm{M}}^{*} \\ \xi \sim (\phi_{\mathrm{M}}^{\mathrm{b}})^{-1/2} & \text{for } \phi_{\mathrm{M}}^{\mathrm{b}} > \phi_{\mathrm{M}}^{*} \end{cases} \tag{16}$$

where the last proportionality for $\phi_{\mathrm{M}}^{\mathrm{b}} > \phi_{\mathrm{M}}^{*}$ is the mean-field scaling in the marginal regime [6, 12]. The crossover concentration between the dilute and marginal regimes is denoted as ϕ_{M}^{*}. It varies with the bonding energy as $\phi_{\mathrm{M}}^{*} \sim \exp(-E/3kT)$ (which is found by equating

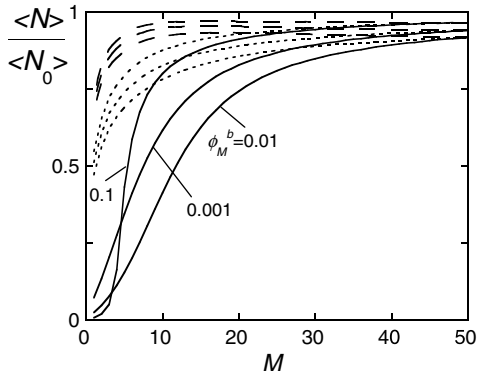

Figure 6. The average chain length (normalized with respect to that in the bulk) as a function of the separation distance for $E = 15kT$ and for three different $\phi_{\mathrm{M}}^{\mathrm{b}}$. Full curves: full equilibrium, broken curves: restricted equilibrium with perfect-slip conditions (constant $\langle\phi_{\mathrm{M}}\rangle$, see section 4.1), dotted curves: restricted equilibrium with no-slip conditions (see section 4.2). At $M' = 50$ the curves of full and restricted equilibrium coincide.

$\langle R_{\mathrm{g}}\rangle$ and ξ). At intermediate concentrations, around ϕ_{M}^{*}, Δ_1 passes through a maximum. The non-monotonic behaviour of Δ_1 can also be seen in figure 3. Note that, for very low concentrations and not very large E, the depletion layer thickness decreases faster with decreasing concentration than predicted by equation (16), because the chains become very short in this case. Also at very high concentrations, deviations from equation (16) are observed. This is due to a crossover from the marginal to the concentrated regime, where higher-order interactions become important [6, 12]. Obviously, in a melt ($\phi_{\mathrm{M}}^{\mathrm{b}} = 1$), $\Delta_1 = 0$.

Upon decreasing the surface separation, the average monomer concentration in the gap decreases monotonically, because it becomes more unfavourable for polymers to be inside the gap, see figure 4. At very small separations ($M \ll \Delta_1$) the polymer concentration in the gap vanishes ($\phi_{\mathrm{M}}(z) \approx 0$ for any z), as can be seen in figure 4. It follows from equation (14) that $\theta^{\mathrm{ex}} = -M\phi_{\mathrm{M}}^{\mathrm{b}}$ in this regime, so that the excess amount varies linearly with M. At intermediate separations, θ^{ex} passes through a minimum at sufficiently high concentrations (e.g. the curve for $\phi_{\mathrm{M}}^{\mathrm{b}} = 0.1$ in figure 3). This minimum has been observed before for monodisperse homopolymers [7, 8, 30]. As discussed in detail in a recent paper, the origin of this minimum is the ordering of individual polymer coils in layers near the surface [30]. For equilibrium polymers the minimum is weaker than for monodisperse polymers, because polydispersity smears out the packing of the polymer coils.

Our results for the dilute regime ($\phi_{\mathrm{M}}^{\mathrm{b}} \ll \phi_{\mathrm{M}}^{*}$) may be compared to those of Schmitt *et al* [22], who derived an analytical expression for $\langle\phi_{\mathrm{M}}\rangle$ for this regime (based on a continuum model for ideal Gaussian chains). Their expression depends only on the ratio $h/\langle R_{\mathrm{g}}\rangle$, with h the surface separation and $\langle R_{\mathrm{g}}\rangle$ the unperturbed radius of gyration of a chain with a length equal to the average length in the bulk. For chains on a cubic lattice without backfolding, $\langle R_{\mathrm{g}}\rangle = \frac{1}{2}l\langle N_0\rangle^{1/2}$ (with l the lattice spacing) [31]. In order to compare with the continuum model, the surfaces must be located in the middle of layers 0 and $M+1$ (see figure 1). Hence, we take $h = (M+1)l$ for the surface separation and $\langle\phi_{\mathrm{M}}\rangle = \sum_z \phi_{\mathrm{M}}(z)/(M+1)$ for the average volume fraction. In this way, we obtain nearly quantitative agreement with Schmitt's results. Small differences between our numerical model and the analytical results of Schmitt *et al* are due to small chains that cannot be described by the continuum model and to subtle differences in the boundary conditions in the two models [32].

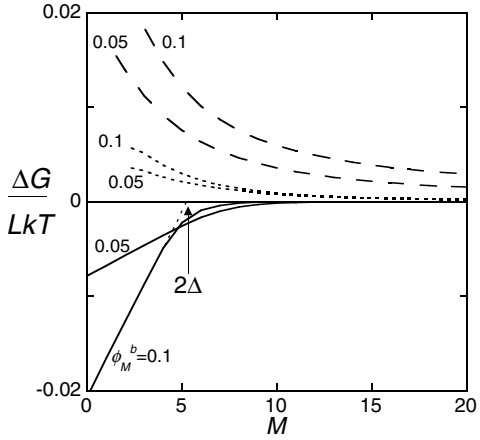

Figure 7. The free energy of interaction between two plates immersed in a solution of living polymers for $E = 15kT$ and several values of ϕ_M^b. Full curves: full equilibrium, broken curves: restricted equilibrium with perfect-slip conditions (constant $\langle\phi_M\rangle$, see section 4.1), dotted curves: restricted equilibrium with no-slip conditions (see section 4.2). $M' = 50$.

The effect of confinement on the average length of the chains is shown in figure 6. Here $\langle N\rangle$ (divided by the average length in the bulk $\langle N_0\rangle$) is shown as a function of the gap size M for $E = 15kT$ and for several values of ϕ_M^b (full curves denote full equilibrium). Clearly, the average chain length inside the gap decreases strongly with decreasing gap width: because the longest chains suffer most from conformational restrictions, they are excluded from the gap first. This effect is strongest for the concentration where the depletion layer thickness has a maximum (around $\phi_M^b = 0.01$ for $E = 15kT$). Again, for dilute solutions our results are in excellent agreement with the results of Schmitt *et al* [22].

The interaction free energy between the two surfaces, given by equation (5), is shown in figure 7 for $E = 15kT$ and several bulk concentrations of monomers (full curves again denote full equilibrium). At large separations, when the depletion layers of the two surfaces do not overlap, $\Delta G = 0$. The volume fraction of monomers in the middle of the gap is equal to that in the bulk in this case (see figure 2(a)), so that the osmotic pressure inside and outside are equal. As the depletion layers begin to overlap, the surfaces start to attract each other, because the osmotic pressure in the gap becomes lower than that in the bulk (the concentration in the middle of the gap is now lower than ϕ_M^b, see figure 2(b)). As a result, the plates are pushed together. For very dilute solutions, our results are again in very good agreement with the analytical results of Schmitt *et al* [22][1].

At short distances, the interaction free energy varies linearly with M. At these separations the polymer concentration (figure 4), and as a result also the osmotic pressure in the gap, vanishes. The effective pressure pushing the plates together (giving the slope of the curves in figure 7) is then equal to the outside osmotic pressure. This can also be seen as follows: if there are no monomers in the gap (i.e. $\theta_M = 0$ and $\theta_S = M$), the only contacts in the gap are between the faces of solvent molecules. From equation (8) it follows that the face weighting factor $G_\alpha^d(z)$ is then equal to unity for solvent faces for all z and d. From equation (11) it follows that $G_S(z) = C$ in this case and equation (10) then gives $C = \Lambda_S^{-1}$. Hence, the interfacial tension (equation (12)) is given by $2\gamma a = kTM \ln C = -M\mu_S$. Since the chemical

[1] Schmitt *et al* give an expression for the disjoining pressure, $p = -\partial(\Delta G)/\partial h$. This expression was compared to our results after numerically differentiating our ΔG.

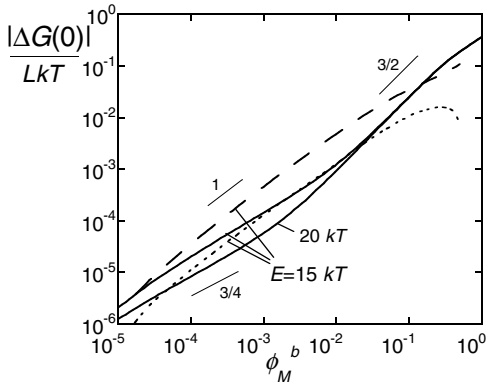

Figure 8. The interaction free energy between the surfaces at zero separation as a function of the bulk concentration for monomers with two different E. Full curves: full equilibrium (depletion attraction), broken curves: restricted equilibrium with perfect-slip conditions (repulsion, see section 4.1), dotted curves: restricted equilibrium with no-slip conditions (repulsion, see section 4.2).

potential of the solvent μ_S is constant under full equilibrium conditions, the interfacial tension, and also the interaction free energy (equation (5)), vary linearly with M. The slope is $-\mu_S$, which is equal to Πv_S according to standard thermodynamics with Π the osmotic pressure and v_S the molecular volume of a solvent molecule (in the present model equal to the volume of one lattice site). Indeed, the slope of the interaction curves is given by the osmotic pressure. At zero separation ($M = 0$) the contribution of the polymers to the interfacial tension is zero (energetic interactions due to direct contact of the surfaces are not considered here). The range of the interaction 2Δ can be obtained by extrapolation of the linear section in ΔG versus M to the abscissa (see figure 7). This is a measure for the gap width where, upon decreasing M, all the polymer is squeezed out of the gap. With this definition for Δ we can write for the interaction free energy at short distances ($M < 2\Delta$)

$$\Delta G(M) = L\Pi v_S(M - 2\Delta). \tag{17}$$

The range and strength of the interaction depend strongly on the monomer concentration. In figure 5 the range of the interaction Δ is shown as a function of the bulk monomer concentration for several values of E (the full curves). Clearly, the range of the attraction follows the same trend as the depletion layer at a single surface Δ_1. The same scaling regimes are found for Δ (equation (16)). The maximum in Δ occurs at slightly higher ϕ_M^b than that in Δ_1.

The depth of the free energy well at zero separation follows from equation (17): $\Delta G(0) = -2A\gamma(\infty) = -2L\Pi v_S\Delta$. We do not consider energetic contributions due to direct contact of the surfaces. The osmotic pressure Π increases with concentration, while the range of the attraction Δ passes through a maximum and then decreases. As shown in figure 8, $-\Delta G(0)$, which is proportional to the product $\Pi\Delta$, increases monotonically with increasing concentration. Hence, the increase of Π is stronger than the decrease of Δ above the overlap concentration.

For the osmotic pressure of a solution of equilibrium polymers in an athermal solvent, the following expression can be derived within the Bethe–Guggenheim approximation for

$E \gg kT$ (see the appendix):

$$\frac{\Pi v_S}{kT} = \frac{q}{(q-2\phi_M^b)}\frac{\phi_M^b}{\langle N_0\rangle} - \ln(1-\phi_M^b) + \frac{q}{2}\ln\left(1-\frac{2\phi_M^b}{q}\right)$$
$$\approx \frac{\phi_M^b}{\langle N_0\rangle} + \left(\frac{1}{2}-\frac{1}{q}\right)(\phi_M^b)^2 + \left(\frac{1}{3}-\frac{4}{3q^2}\right)(\phi_M^b)^3 + \cdots. \tag{18}$$

This equation is similar to the Flory–Huggins expression for the osmotic pressure of polydisperse polymer solutions [20] with corrections that arise from the correlations between the occupation of neighbouring sites. For dilute solutions ($\phi_M^b \ll 1/\langle N_0\rangle$) equation (18) reduces to Van't Hoff's law for ideal solutions: $\Pi v_S/kT \approx \phi_M^b/\langle N_0\rangle = (\phi_M^b)^{1/2}\exp(-E/2kT)$ (with $\phi_M^b/\langle N_0\rangle$ the number concentration of chains). Above the overlap concentration, in the marginal regime ($1/\langle N_0\rangle \ll \phi_M^b \ll 1$), $\Pi v_S/kT \sim (\phi_M^b)^2$. Combining this with equation (16) we find

$$-\Delta G(0) \sim \begin{cases} (\phi_M^b)^{3/4}\exp\left(\dfrac{-E}{4kT}\right) & \text{for } \phi_M^b < \phi_M^* \\ (\phi_M^b)^{3/2} & \text{for } \phi_M^b > \phi_M^*. \end{cases} \tag{19}$$

The depth of the interaction well increases monotonically with increasing concentration. In dilute solutions it becomes weaker if the bonding energy increases, while above the overlap concentration it is independent of the bonding energy. The scaling regimes with concentration are indicated in figure 8. For very low concentrations and relatively small bonding energies the chains are very short and there is hardly any depletion. In this case the attraction decreases faster with decreasing concentration than predicted by equation (19). Also at very high concentrations deviations occur from equation (19) because higher-order terms in the expansion of equation (18) become important, and also the correlation length decreases faster with concentration in the concentrated regime (see figure 5).

We note that in [25] we introduced an alternative measure for the depletion layer thickness, based on the shape of the volume fraction profile at a single surface. At large z, the volume fraction approaches the bulk value exponentially: $\phi_M^b - \phi_M(z) \sim \exp(-z/\Delta_2)$. It was shown that the decay length Δ_2 may be used as an alternative measure for the depletion layer thickness, which behaves in qualitatively the same manner as Δ and Δ_1. Similarly, the interaction free energy $\Delta G(M)$ between two surfaces decays exponentially to zero at large separations: $-\Delta G(M) \sim \exp(-M/\Delta_2)$. The decay length is the same as that of the concentration profile at a single surface.

4. Restricted equilibrium

In the previous section we have discussed depletion interactions under conditions of full equilibrium between the interior of the gap between the surfaces and a bulk solution. For this situation to occur, the molecules in the gap should be able to diffuse out of the gap on the timescale of the variation of the distance between the two surfaces. For a relatively fast approach of two surfaces of large area this is not likely to be the case, especially at small separations. Full equilibrium between the gap and the bulk cannot be maintained for such cases and the chemical potential in the gap differs from that in the bulk. In order to be able to describe this situation, we need to make assumptions about the amount of polymer in the gap. Here we assume that, for separations $M < M'$, the amount of polymer in the gap varies only because of the fluid flow induced by the movement of the surfaces (here M' may be considered as the starting point of the compression of the gap; for $M \geqslant M'$ full equilibrium is maintained). Diffusion of polymer from the gap to the bulk and vice versa is completely

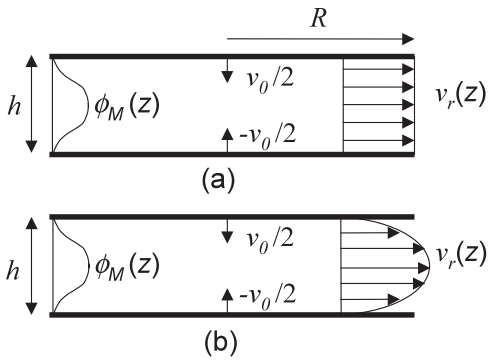

Figure 9. Schematic representation of two different cases of restricted equilibrium. The two surfaces approach each other with a velocity v_0. (a) Perfect-slip conditions, corresponding to a fluid velocity v_r independent of z. (b) No-slip conditions, corresponding to a parabolic velocity profile v_r. In both cases, the concentration profile in the normal direction $\phi_M(z)$ (left) is always at a local equilibrium.

neglected for $M < M'$. The monomer concentration in the gap is then completely determined by the flow profile of the fluid that is squeezed out of the gap upon the approach of the surfaces (see figure 9). We assume furthermore that local equilibrium is maintained in the direction normal to the surfaces. These assumptions are reasonable for a narrow gap between two large surfaces, for which the distance over which the polymers have to diffuse is much larger in the lateral direction than in the normal direction.

In order to calculate the amount of monomers in the gap at every separation, we need to make an assumption about the velocity profile of the fluid flow out of the gap as the surfaces are brought closer together. This profile depends on the slip conditions at the wall. Two limiting cases will be considered. In section 4.1 we consider the case of perfect slip at the walls. This corresponds to a radial velocity which is independent of the distance to the surfaces (figure 9(a)). In section 4.2 we consider the case of no slip at the walls. This corresponds to a parabolic velocity profile in the direction parallel to the surfaces (figure 9(b)). In reality the flow profile lies probably in between these two limiting cases. In the depletion zones near the two surfaces the viscosity is lower than in the middle of the gap due to the lower polymer concentration. This results in a higher shear rate in the depletion zones. This effect becomes larger if the polymer concentration becomes higher, because the difference in viscosity is larger then. Hence, we may expect that with increasing concentration we go from no-slip to perfect-slip conditions.

4.1. Perfect slip: constant average monomer concentration

The simplest approach is to assume that perfect slip occurs at the walls, i.e. all the shear occurs at the walls. This results in a fluid velocity in the direction parallel to the surfaces which is independent of the distance to the surfaces (a block profile, see figure 9(a)). The solution that flows out of the gap in this case has a polymer concentration equal to the average concentration in the gap. The average concentration in the gap $\langle\phi_M\rangle$ then remains constant for all separations $M < M'$. At the starting point $M = M'$ the gap is in full equilibrium with the bulk, so that $\langle\phi_M\rangle$ is related to the bulk concentration by $\langle\phi_M\rangle = \phi_M^b + \theta_{fe}^{ex}(M')/M'$ (see equation (14)), where $\theta_{fe}^{ex}(M')$ is the excess amount of monomers at a separation M' under full equilibrium conditions. Since $\theta_{fe}^{ex}(M')$ is negative for the present case of nonadsorbing polymers

(see figure 3), $\langle\phi_M\rangle < \phi_M^b$. Here we take M' arbitrarily equal to 50 lattice layers. The amount of monomers in the gap for $M < M'$ varies as $\theta_M = M\langle\phi_M\rangle$. The chemical potential, which is no longer constant, can be found from equation (10). (For details about the calculation method, see [26].)

The broken curves in figure 6 show the variation of the average length of the chains with surface separation for this situation for three values of ϕ_M^b. As a result of the fixed monomer concentration the average length varies only very little with decreasing M. At $M = M' = 50$, where the gap is in full equilibrium with the bulk, the average length is slightly smaller than that in the bulk. As the surface separation decreases, the average length first increases slightly. At intermediate distance it passes through a (weak) maximum, and at very small separations the average length decreases somewhat upon decreasing M. The initial increase of $\langle N\rangle$ with decreasing M is a result of the concentration profile (see figure 2(a)): as a result of the depletion layers near the surfaces, the monomer concentration in the middle of the gap increases as M becomes smaller (in order to keep the average monomer concentration in the gap constant). Since the average length depends on the concentration (equation (2)), this elevation of the local concentration causes a slight increase of the average length. At very small separations the chain length decreases again, because of conformational restrictions. The conformational entropy of a bond between two monomers in a narrow gap is smaller than that in a homogeneous system, because the surfaces exclude some directions for bond formation. This may be considered as an effective decrease of the bonding free energy as compared to chains in a homogeneous solution. In a slit of one lattice layer on a cubic lattice there are only three possible directions for every next bond rather than five in the bulk (two directions are excluded by the presence of the surfaces). Hence, the conformational entropy of a bond is reduced by an amount $k\ln(5/3)$ and the (absolute value of the) effective bonding free energy is smaller by an amount $kT\ln(5/3)$. From equation (2) we see that the average length in a slit of one layer is then smaller by a factor of $\sqrt{5/3}$ compared to a homogeneous 3D system of the same monomer concentration.

The broken curves in figure 7 represent the interaction free energy between the two surfaces for a constant average monomer concentration for $E = 15kT$ and several ϕ_M^b. It is clear that the equilibrium polymers trapped between the two surfaces in the gap cause repulsion between the surfaces. This was also found by Schmitt *et al* [22] for ideal equilibrium polymers without excluded volume interactions. The interaction free energy extrapolated to zero separation is shown in figure 8 (broken curves). With increasing monomer concentration the repulsion becomes stronger. For not too high concentrations $\Delta G(0)$ increases proportionally to ϕ_M^b. Results are presented only for $E = 15kT$. For other values of E, the strength of the repulsion is nearly the same. Hence, $\Delta G(0)$ depends only weakly on the bonding energy E.

The repulsion is a result of the decrease of conformational entropy of the confined chains. As explained above, the conformational entropy of a bond in a gap of one lattice layer is lower by an amount $k\ln(5/3)$ as compared to that of a bond in the bulk. For high enough bonding energy and monomer concentration (when the average length is much larger than unity) almost all bonding groups of the monomers are linked to another bonding group. Hence, the number of bonds is almost equal to the number of monomers. It follows that the total difference in conformational entropy per lattice site between monomers confined in a slit of one lattice layer and monomers in the bulk is approximately equal to $\Delta S^c/L \approx -k\phi_M^b\ln(5/3)$ (where we have neglected the difference between $\langle\phi_M\rangle$ and ϕ_M^b and the effect of confinement on the chain length distribution). This may be used as an estimate for the strength of the interaction at zero separation: $\Delta G(0) \approx -T\Delta S^c \approx kTL\phi_M^b\ln(5/3)$. Indeed, it increases proportionally to ϕ_M^b and does not depend on E. For high concentrations, deviations from this scaling are seen, and also for small E and very low ϕ_M^b (when $\langle N_0\rangle$ is of the order of unity) the interaction is weaker.

4.2. No slip: outflow with parabolic velocity profile

In the previous section we assumed perfect slip at the walls, which results in a radial velocity which is independent of the z coordinate (figure 9(a)) and in an average volume fraction in the gap that remains constant upon compression of the gap. If there is no perfect slip at the walls, however, the radial velocity will be higher in the middle of the gap than close to the walls (figure 9(b)). Because the monomer concentration is also highest in the middle of the gap, the average concentration of the solution that flows out of the gap will be higher than the average concentration in the gap. Here, we consider the other limiting case, when there is no slip at the walls (the velocity in the parallel direction is then zero at the two surfaces). For simplicity, we consider two parallel circular plates of radius R (and area $A = \pi R^2$). We begin with the surfaces far apart ($M = M'$ or $h = h'$). When the plates are brought closer together, fluid is squeezed out of the gap. For a narrow gap between two large plates ($R \gg h$) and for small velocities the velocity profile of the fluid flow has been calculated by Reynolds [33]. In the radial direction, parallel to the surfaces, the velocity is

$$v_{\mathrm{r}}(r, \hat{z}) = \frac{3r\hat{z}[h - \hat{z}]v_0}{h^3} \tag{20}$$

and in the normal direction, perpendicular to the surfaces:

$$v_z(r, \hat{z}) = \frac{6\left[\hat{z}^2\left(\frac{\hat{z}}{3} - \frac{h}{2}\right) + \frac{h^3}{12}\right]v_0}{h^3}. \tag{21}$$

Here r is the distance from the centre of the gap in the direction parallel to the surfaces and $\hat{z}$ is the distance in the normal direction from the lower surface. Expressed in terms of the lattice model, $\hat{z} = l(z - \frac{1}{2})$ with l the lattice spacing (see figure 1). The velocity at which the plates approach each other is $v_0 = \mathrm{d}h/\mathrm{d}t$. At the walls ($\hat{z} = 0$ and h), the velocity in the radial direction v_{r} equals zero, while the normal velocity v_z is equal to $\pm v_0/2$ (the normal velocity is measured relative to the position of the middle of the gap). In the middle of the gap ($\hat{z} = h/2$), the radial velocity has a maximum (which depends on the radial coordinate r) and the normal velocity is zero. Because the normal velocity does not depend on the r coordinate, and because there is no concentration gradient in the r direction at the beginning, the concentration in the lateral direction remains homogeneous. The amount of molecules of type A that flow out of the gap at the edge ($r = R$) in a time $\mathrm{d}t$ (corresponding to a change in separation $\mathrm{d}h$) is then

$$\mathrm{d}n_{\mathrm{A}}^{\mathrm{g}} = -2\pi R\,\mathrm{d}t \int_0^{h(t)} v_{\mathrm{r}}(R, \hat{z})\phi_{\mathrm{A}}(z)\,\mathrm{d}\hat{z} \tag{22}$$

where $\phi_{\mathrm{A}}(z)$ is the volume fraction of component A at coordinate z. The corresponding change in the average volume fraction is $\mathrm{d}\langle\phi_{\mathrm{A}}^{\mathrm{g}}\rangle = \mathrm{d}n_{\mathrm{A}}^{\mathrm{g}}/(\pi R^2 h)$. We assume that at every separation distance h the volume fraction profile $\phi_{\mathrm{A}}(z)$ maintains a local equilibrium.

We start again at a separation M' equal to 50 lattice layers ($h = M'l = 50l$), for which the profile is in full equilibrium with the bulk. Then we decrease the separation by one lattice layer ($\mathrm{d}h = l$) and calculate the new amount of polymer using equations (20) and (22). The concentration profile in the normal direction is allowed to reach a new local equilibrium for the given amount of polymer and then h is reduced again by one layer, and so on. This procedure resembles a typical experiment with a surface force apparatus.

The dotted curves in figure 4 show the resulting average volume fraction in the gap as a function of the separation distance for $E = 15kT$ and several $\phi_{\mathrm{M}}^{\mathrm{b}}$. In figure 3 the corresponding excess amount is shown (dotted curves). For $M > M' = 50$, the curves of restricted equilibrium and full equilibrium coincide, by definition. Because the flow velocity is largest where the monomer concentration is highest, the fluid that leaves the gap has a

monomer concentration that is higher than the average concentration in the gap. As a result, the average concentration in the gap decreases with decreasing surface separation. The monomer concentration in the gap is higher than the equilibrium value (full curves), however, and the excess amount in the gap changes more smoothly than for full equilibrium.

The average length of the chains for restricted equilibrium with a parabolic flow profile is shown in figure 6 (the dotted curves). The average length decreases monotonically with decreasing surface separation. This decrease is faster than for a constant average volume fraction (the broken curves), but slower than for full equilibrium conditions (the full curves). This trend follows the variation of the average monomer concentration in the gap: the lower $\langle\phi_M\rangle$, the smaller the average length.

The interaction between the two surfaces is also shown in figure 7 (the dotted curves). The interaction is again repulsive, but this repulsion is weaker than for the case of a constant average volume fraction in the gap, because the polymer concentration in the gap is closer to the equilibrium value (see figure 4). The repulsion becomes stronger for increasing concentration, as shown in figure 8 (the dotted curves). Again, the effect of the bonding energy on $\Delta G(0)$ is very weak.

Under restricted equilibrium conditions, one generally encounters hysteresis effects. The force measured upon a decrease of the separation h (compression of the gap) differs from the force measured upon an increase of h (expansion of the gap). The reason for this hysteresis is that the composition of the fluid flow out of the gap upon a decrease of h is different from that of the flow into the gap when h increases. The latter will have a composition which is more or less equal to the bulk composition. Since the fluid flows into the gap only at the edge of the gap, the local concentration at the edge may become different than that in the middle of the gap. Because of this complication, we will not consider the interaction upon an increase of h here.

5. Concluding remarks

In this paper we have considered equilibrium polymers confined between two surfaces. The average concentration in the gap, the average length of the chains and the interaction between the surfaces were considered. When the gap is in full equilibrium with the bulk of the solution, the equilibrium polymers cause depletion attraction. The range of this attraction, which is related to the depletion layer thickness at a single surface, passes through a maximum as a function of concentration. In dilute solutions it corresponds to the average radius of gyration of the chains, which increases with concentration, while above the overlap concentration it corresponds to the correlation length, which decreases with concentration. The strength of the attraction increases monotonically with concentration.

When the diffusion of polymers between the gap and the bulk is too slow to maintain full equilibrium, the situation changes. The amount of polymer in the gap is no longer determined by thermodynamic equilibrium with the bulk, but by the flow of fluid out of the gap upon compression of the gap. Two limiting cases were considered: that of perfect slip at the walls and that of no slip at the walls. In both cases, the interaction between the surfaces becomes repulsive.

Schmitt *et al* [22] and Rouault and Milchev [24] used a different boundary condition for restricted equilibrium. They assumed that both the average volume fraction in the gap and the total volume of the gap remain constant. Hence, as the surfaces move closer together (h decreases), the area of the surfaces increases proportionally, such as to keep $V = Ah$ constant. This situation may be relevant for the spreading of a thin film deposited on a solid substrate. The average length of the chains in the gap for this case is the same as the broken curves in figure 6. In the calculation of the interaction free energy, however, the change of

the area A in equation (3) should be taken into account and the bulk terms must be omitted. Lattice calculations for this case (not shown) indicate that this leads to a repulsion very similar to those shown in figure 5 for constant $\langle\phi_M\rangle$ and A.

Experimental evidence for interactions between surfaces in the presence of equilibrium polymers is scarce. Kékicheff *et al* [27] measured depletion interactions between two mica surfaces in semi-dilute solutions of wormlike micelles of CTAB. They measured an attraction with a range that decreased with concentration as $\Delta \sim \phi^{-0.65}$. The exponent is somewhat larger than the mean-field exponent $1/2$ and somewhat smaller than the semi-dilute exponent $3/4$. No measurements in the dilute regime have been reported. Interactions under restricted equilibrium can be measured by decreasing the timescale of the experiment (reducing the waiting time in a surface force apparatus or increasing the drive frequency in an atomic force microscope).

Appendix. Osmotic pressure of a solution of equilibrium polymers

From standard thermodynamics, we know that the osmotic pressure of a solution is related to the chemical potential of the solvent: $\Pi v_S = -\mu_S$. The chemical potential in its turn is related to the monomer concentration and the weighting factor G_S by equation (9). Hence

$$\frac{\Pi v_S}{kT} = -\frac{\mu_S}{kT} = -\ln(1-\phi_M) - \ln(G_S). \tag{A.1}$$

The weighting factor of a solvent molecule is related to the face weighting factor by equation (11): $G_S = (G_0^d)^q$, where the subscript 0 denotes a face of a solvent molecule. Similarly, we denote the bonding groups of the monomers as faces of type 2 and the $q-2$ remaining faces of the monomers as faces of type 1. The face weighting factors G_α^d follow from equations (7) and (8). In a homogeneous isotropic solution (all site fractions are the same for all layers z and directions d) this gives

$$\phi_0^d = \frac{(\phi_0^d)^2}{(G_0^d)^2} + \frac{\phi_0^d\phi_1^d}{G_0^dG_1^d} + \frac{\phi_0^d\phi_2^d}{G_0^dG_2^d} \tag{A.2}$$

$$\phi_1^d = \frac{\phi_1^d\phi_0^d}{G_1^dG_0^d} + \frac{(\phi_1^d)^2}{(G_1^d)^2} + \frac{\phi_1^d\phi_2^d}{G_1^dG_2^d} \tag{A.3}$$

$$\phi_2^d = \frac{\phi_2^d\phi_0^d}{G_2^dG_0^d} + \frac{\phi_2^d\phi_1^d}{G_2^dG_1^d} + \frac{(\phi_2^d)^2}{(G_2^d)^2}\mathrm{e}^{E/kT} \tag{A.4}$$

where we have used $\phi_\alpha^d = \phi_\alpha^{-d}$ and $G_\alpha^d = G_\alpha^{-d}$. The site fractions of faces ϕ_α^d are related to the concentration of monomers:

$$\phi_0^d = 1-\phi_M \tag{A.5}$$

$$\phi_1^d = \frac{(q-2)\phi_M}{q} \tag{A.6}$$

$$\phi_2^d = \frac{q\phi_M}{2}. \tag{A.7}$$

Equations (A.2)–(A.7) can be solved exactly for G_0^d, G_1^d and G_2^d as a function of ϕ_M and E. With equation (2) we obtain G_0^d as a function of ϕ_M and $\langle N_0\rangle$. The full expression is too long to display here, but for $E \gg kT$ it reduces to

$$G_0^d \approx \sqrt{1-\frac{2\phi_M}{q}} + \frac{\phi_M}{\langle N_0\rangle\sqrt{q^2-2\phi_M q}}. \tag{A.8}$$

Equation (11) then gives the monomer weighting factor G_S, which can be substituted in equation (A.1) to yield an expression for the osmotic pressure as a function of ϕ_M and $\langle N_0 \rangle$. Expanding in terms of $\phi_M/\langle N_0 \rangle$ and neglecting second- and higher-order terms then gives equation (18).

References

[1] Asakura S and Oosawa F 1954 *J. Chem. Phys.* **22** 1255
[2] Asakura S and Oosawa F 1958 *J. Polym. Sci.* **33** 183
[3] De Gennes P G 1979 *Scaling Concepts in Polymer Physics* (Ithaca, NY: Cornell University Press)
[4] Joanny J F, Leibler L and De Gennes P G 1979 *J. Pol. Sci. Pol. Phys. Edn* **17** 1073
[5] Feigin R I and Napper D H 1981 *J. Colloid Interface Sci.* **75** 525
[6] Fleer G J, Cohen Stuart M A, Scheutjens J M H M, Cosgrove T and Vincent B 1993 *Polymers at Interfaces* (London: Chapman and Hall)
[7] Fleer G J and Scheutjens J M H M 1987 *Croatica Chem. Acta* **60** 477
[8] Scheutjens J M H M and Fleer G J 1982 *Adv. Colloid Interface Sci.* **16** 361
[9] Tadros T F 1982 *The Effect of Polymers on Dispersion Properties* ed T F Tadros (New York: Academic) p 1
[10] Yarar B 1982 *Solution Behavior of Surfactants* ed K L Mittal and E J Fendler (New York: Plenum) p 1333
[11] Napper D H 1983 *Polymeric Stabilization of Colloidal Dispersions* (London: Academic)
[12] Grosberg A Y and Khokhlov A R 1994 *Statistical Physics of Macromolecules* (New York: American Institute of Physics)
[13] Roefs S P F M, Scheutjens J M H M and Leermakers F A M 1994 *Macromolecules* **27** 4810
[14] Hariharan A, Kumar S K and Russell T P 1990 *Macromolecules* **23** 3584
[15] Van der Gucht J, Besseling N A M and Fleer G J 2002 *Macromolecules* **35** 6732
[16] Cates M E and Candau S J 1990 *J. Phys.: Condens. Matter* **2** 6869
[17] Sijbesma R P, Beijer F H, Brunsveld L, Folmer B J B, Hirschberg J H K K, Lange R F M, Lowe J K L and Meijer E W 1997 *Science* **278** 1601
[18] Boileau S, Bouteiler L, Lauprêtre F and Lortie F 2000 *New J. Chem.* **24** 845–8
[19] Fogleman E A, Yount W C, Xu J and Craig S L 2002 *Angew. Chem. Int. Edn.* **41** 4026
[20] Flory P J 1953 *Principles of Polymer Chemistry* (Ithaca, NY: Cornell University Press)
[21] Flory P J 1936 *J. Am. Chem. Soc.* **58** 1877
[22] Schmitt V, Lequeux F and Marques C M 1993 *J. Physique* **3** 891
[23] Milchev A and Landau D P 1996 *J. Chem. Phys.* **104** 9161
[24] Rouault Y and Milchev A 1997 *Macromol. Theor. Simul.* **6** 1177
[25] Van der Gucht J and Besseling N A M 2002 *Phys. Rev.* E **55** 051801
[26] Besseling N A M and Scheutjens J M H M 1994 *J. Phys. Chem.* **98** 11597
[27] Kékicheff P, Nallet F and Richetti P 1994 *J. Physique* **4** 735
[28] Besseling N A M and Lyklema J 1994 *J. Phys. Chem.* **98** 11610
[29] Besseling N A M 1997 *Langmuir* **13** 2113
[30] Van der Gucht J, Besseling N A M, Van Male J and Cohen Stuart M A 2000 *J. Chem. Phys.* **113** 2886
[31] Yamakawa H 1971 *Modern Theory of Polymer Solutions* (New York: Harper and Row)
[32] Gorbunov A A, Skvortsov A M, Van Male J and Fleer G J 2001 *J. Chem. Phys.* **114** 5366
[33] Reynolds O 1886 *Phil. Trans. R. Soc.* A **177** 157